A Novel Grid-connected Harmonic Current Suppression Control for Autonomous Current Sharing Controller-based AC Microgrids

Yajuan Guan
Research Programme on Microgrids
Department of Energy Technology,
Aalborg University
Aalborg, Denmark
ygu@et.aau.dk

Wei Feng
State Key Lab of Power Systems,
Department of Electrical Engineering,
Tsinghua University
Bejing, China
fwqqrse@163.com

Jinghang Lu, Josep M. Guerrero, Juan C. Vasquez
Research Programme on Microgrids
Department of Energy Technology,
Aalborg University
Aalborg, Denmark
{jgl, joz, juq}@et.aau.dk

***Abstract*—Since the power quality of feed-in grid current in a grid-connected microgrid (GCMG) can be influenced by a distorted utility grid, a novel feed-in grid harmonic current suppression control strategy is proposed in this paper. A feed-in grid current resonant controller-based harmonic compensation loop is integrated to the original autonomous current sharing controller. The feed-in grid harmonic current compensation loop that cooperated with the parallel resonant controllers in voltage control loop can effectively reduce the system equivalent output admittance at selected harmonic frequencies. Thus, the total harmonic distortion of feed-in grid current can be significantly decreased. Simulation and experimental results from a three-voltage-controlled-inverter-based GCMG verify the effectiveness of the proposed controller.**

Keywords—Feed-in grid harmonic current suppression, resonant control, autonomous current sharing controller, grid-connected microgrid.

I. INTRODUCTION

At present, microgrids (MGs) are considered promising electric power systems with decentralized power architectures because of its capability to integrate various kinds of renewable energy sources and power electronics interfaced with distributed generation units (DGs) [1]. The widespread use of interfacing inverters for DG units may result in harmonic interaction or even lead to resonances in MGs. In addition, the presence of nonlinear loads, passive harmonic filters, and parasitic capacitors in distribution feeders may also induce a harmonic current and low-order harmonic resonance [2].

When an MG operates in the islanded mode, the power quality issue focuses on keeping the output voltage harmonic components within desired limitations, and on proportionally sharing harmonic currents among the paralleled inverters. A number of studies have been published to address these issues [3]–[6]. In [3] and [4], the G–H and Q−–G droop controls are used to share harmonics and unbalanced currents among DG units. An enhanced virtual impedance control scheme for islanded MGs at fundamental and selected harmonic frequencies is proposed in [5]. A power-harmonic conductance droop is presented in [6]. However, since the RMS values of total active and reactive harmonic power are usually used, different sequences and orders of harmonic components cannot be controlled separately.

The power quality issues will become more complicated when an MG operates in grid-connected mode because the output impedance of a grid-connected MG (GCMG) is usually small by using the proportional-resonant (PR) voltage controllers; thus, it is easily affected by nonlinear local loads or distorted utility grid [7], [8]. Some novel control principles for grid-connected voltage controlled inverters (GC-VCIs) were proposed in [9]-[12], in which parallel-resonant controllers were used in the voltage control loop to reduce the feed-in grid harmonic current of the GC-VCIs. Furthermore, different harmonic voltage components of the utility grid were extracted by using slide discrete Fourier transformation. Moreover, a closed-loop triple-loop control algorithm was proposed in [13].

The aforementioned control strategies were all developed based on power droop control, which has a relatively slow transient response caused by low-pass filters [14], and small stability margin during droop coefficient variations and voltage reference changes [15]. Therefore, an autonomous current sharing controller (ACSC) [16] for the parallel voltage-controlled inverters (VCIs) is proposed to obtain a fast transient response and large stability margin compared with the conventional power droop control. The corresponding hierarchical control strategy for an ACSC-based MG in grid-connected mode was investigated in [17]. However, in that case, only stiff utility grid is considered.

In this paper, an ACSC-based novel feed-in grid harmonic current suppression control strategy for GCMGs is proposed. A current resonant controller-based feed-in grid harmonic current compensation loop is integrated to the original ACSC. The compensation loop cooperated with the parallel resonant controllers in voltage control loop can effectively reduce the system equivalent output admittance at selected harmonic frequencies. Thus, the total harmonic distortion of feed-in grid current can be significantly decreased. Simulation and experimental results from a three 2.2 kW VCIs-based GCMG are shown to verify the effectiveness of the proposed controller.

This paper is organized as follows. The control principle of ACSC is briefly reviewed in Section II. Section III describes the proposed feed-in grid harmonic current suppression control strategy and analyzes its steady-state control performance. The simulation and experimental results are presented in Section IV. Section V concludes the paper.

978-1-4799-7312-5/18/$31.00 ©2018 IEEE

II. Brief Review of Autonomous Current Sharing Control Strategy

The ACSC used at the primary level is depicted in Fig. 1. The controller includes a synchronous-reference-frame (SRF) virtual resistance (VR) loop (R_{vird} and R_{virq}), an SRF phase-locked loop (PLL), a DC link voltage feed-forward loop, and proportional + resonant (PR) inner voltage and current controllers (G_v and G_i). Inductive currents and capacitor voltages are transformed to the stationary reference frame ($i_{L\alpha\beta}$ and $v_{c\alpha\beta}$). Output currents are transformed to the SRF (i_{odq}). The direct and quadrature current outputs are independently controlled by the SRF-VR loop in dq axis. The inner voltage and current loops are implemented in $\alpha\beta$ frame. The power circuit consists of a three-leg three-phase VCI connected to a DC link, loaded by an L_f-C_f filter, and connected to the AC bus through a power line (Z_{line}).

The proposed controller provides a voltage reference to the inner loop. The voltage reference $\boldsymbol{V}_{ref}$ is generated by combining the amplitude reference ($|\boldsymbol{V}_{ref}|$) and the phase generated (θ) by the SRF-PLL.

In the case of supplying active loads, the direct current flowing through the SRF-VR will drop the direct voltage, causing a decrease in the output voltage amplitude. Hence, a droop characteristic is also imposed by the SRF-VR adapting the amplitude of output voltage, which endows to the system an I_{od}–V droop characteristic.

Even though the PLL is trying to synchronize the inverter with common AC bus, in the case of supplying reactive loads, the quadrature current flowing through the SRF-VR will produce an unavoidable quadrature voltage drop, which will cause an increase in SRF-PLL frequency. Thus, the mechanism inherently endows an I_{oq}-ω droop characteristic in each inverter.

The I_{oq}-ω and I_{od}–V droop characteristics in each inverter are used instead of adopting power droop controller. The relationship of I_{od}, I_{oq}, R_{vird}, and R_{virq} can be generalized and expressed for a number N of converters as follows:

$$I_{od1}R_{vird1} = I_{od2}R_{vird2} = \cdots = I_{odN}R_{virdN} \tag{1a}$$

$$I_{oq1}R_{virq1} = I_{oq2}R_{virq2} = \cdots = I_{oqN}R_{virqN} \tag{1b}$$

The d- and q-axis current outputs I_{od} and I_{oq} of the paralleled inverters are inversely proportional to the corresponding VRs. Therefore, the direct and quadrature current outputs of each inverter can be regulated independently by adjusting the SRF-VRs based on different power rates, commands from central energy management system or other higher level control loops. Furthermore, the active and reactive power outputs sharing strategy among the paralleled inverters can be obtained from (1) by multiplying the voltage reference. Considering that the voltage references (V_{ref}) of each inverter are equal, the active and reactive power outputs will also be properly shared based on the SRF-VRs, as shown in the following relationships:

$$P_{o1}R_{vird1} = P_{o2}R_{vird2} = \ldots = P_{oN}R_{virdN} \tag{2a}$$

$$Q_{o1}R_{virq1} = Q_{o2}R_{virq2} = \ldots = Q_{oN}R_{virqN} \tag{2b}$$

where P_{on} and Q_{on} are the active and reactive power outputs of inverter #n, n = 1, 2, …, N.

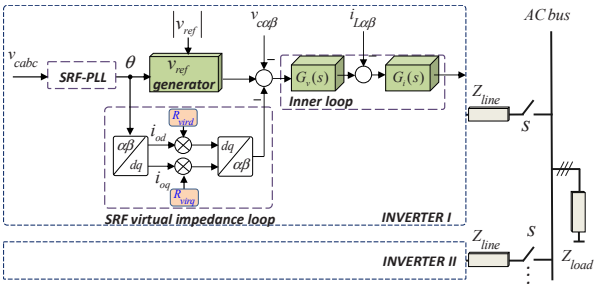

Fig. 1. Autonomous current-sharing control strategy.

III. Proposed Feed-in Grid Harmonic Current Suppression Control Strategy

The GCMG is controlled on the basis of MG hierarchical control theory that is divided into three levels, as shown in Fig. 2. At the primary level, the ACSC is used to realize the current sharing among the paralleled VCIs. At the secondary level, frequency and magnitude synchronization loops are included to guarantee the synchronization between the MG output voltage and the voltage of point of common coupling (PCC) before connecting to the main grid. The tertiary control is used for power flow management.

A. Proposed Feed-in Grid Harmonic Current compensator

To suppress the feed-in grid harmonic current components when a GCMG is connected to a distorted utility grid, the MG common bus voltage must be regulated in accordance with the utility grid voltage. The feed-in grid current of the GCMG is measured and then sent to the primary controller through a low-bandwidth communication link. The measured feed-in grid current is transferred to a stationary reference frame. An additional feed-in grid harmonic current compensator $G_{hi}(s)$, which consists of parallel current resonant controllers, is added at the primary level, as follows:

$$G_{hi}(s) = \sum_{n=5,7,11\ldots} \frac{k_{hi}^{nth} s}{s^2 + (n\omega_b)^2} \tag{3}$$

where k_{hi}^{nth} is the resonant term of the current resonant controller at nth resonant frequency, and ω_b is the fundamental angular frequency.

As presented in Fig. 2, the ultimate voltage reference of a VCI consists of the calculated feed-in grid harmonic current suppression voltage offset $v_{\alpha\beta}^{h}$, the original voltage reference $v_{\alpha\beta}^{ref}$, and $v_{\alpha\beta}^{vr}$ generated by the SFR-VR loop. Meanwhile, the harmonic voltage tracking capability also has to be considered.

The harmonic components in the VCI output voltage should follow the offset $v_{\alpha\beta}^{h}$ precisely to diminish the corresponding harmonic components in feed-in grid current. In this sense, the parallel voltage resonant controllers are adopted in the voltage control loop, as follows:

$$G_v(s) = k_{pv} + \sum_{n=1,5,7,11\ldots} \frac{k_{iv}^{nth} s}{s^2 + (n\omega_b)^2} \tag{4}$$

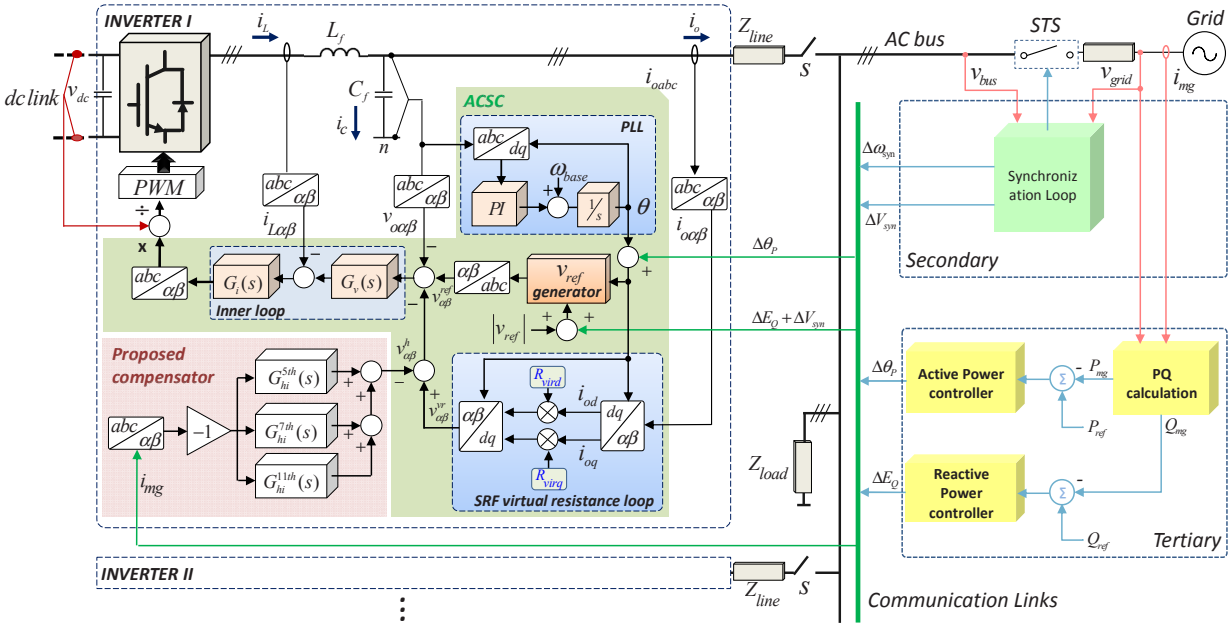

Fig. 2. Overview of the proposed feed-in grid harmonic current suppression controller.

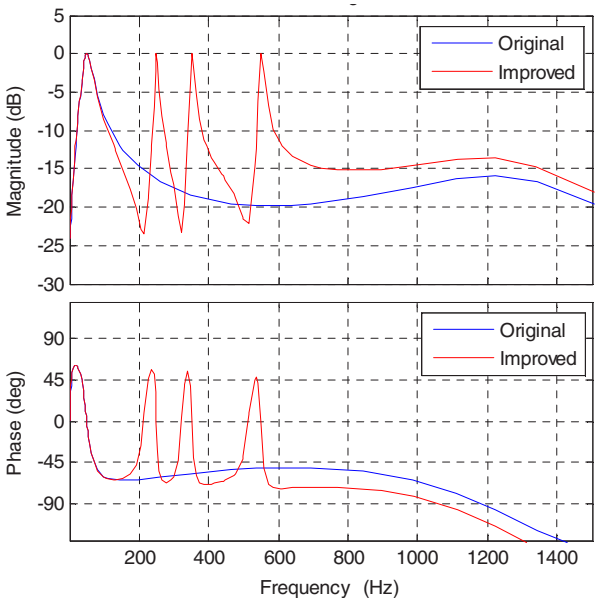

Fig. 3. Comparative Bode diagrams of the VCI with original and improved ACSC.

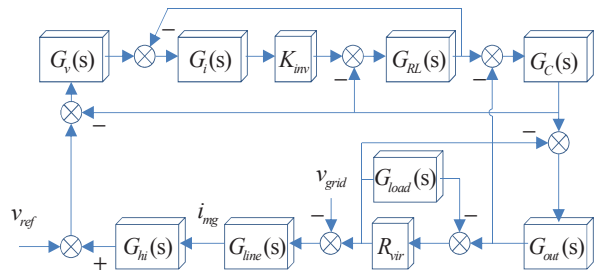

Fig. 4. Equivalent transfer function block model of a GCMG.

where k_{pv} is the proportional term, and k_{iv}^{nth} is the resonant term at the n^{th} resonant frequency. The comparative magnitude-frequency bode diagrams of the VCI with only the conventional ACSC and with the proposed controller are shown in Fig. 3. Obviously, the harmonic voltage tracking capability of VCI can be guaranteed with the proposed control method.

B. Steady-state performance analysis

To analyze the proposed control principle and estimate the steady-state control performance of the proposed feed-in grid harmonic current suppression compensator, an equivalent transfer function is derived as shown in Fig. 4, in which virtual resistance loop and the PLL of ACSC are assumed to be effective for simplicity. The voltage and current controllers of the ACSC are presented as $G_v(s)$ and $G_i(s)$, respectively. VCI is equivalent to a proportional constant K_{inv}. The LC filter is noted as $G_{LR}(s)$ and $G_C(s)$. $G_{out}(s)$ describes the output impedance of VCI. $G_{load}(s)$ represents local sensitive loads. $G_{hi}(s)$ is the proposed feed-in grid harmonic current suppression compensator. The MG is connected to the utility grid through line impedance $G_{line}(s)$. A virtual infinite resistor R_{vir} is added to facilitate the derivation of MG common bus voltage. As a result, the block diagram of the system transfer function can be equivalent to a multiple-input single-output (MISO) system with the voltage reference (v_{ref}) and disturbance voltage (v_{grid}) as the inputs, and feed-in grid current (i_{mg}) as the output. The influence of the distorted grid voltage on feed-in grid current can be estimated by the admittance characteristic at harmonic frequencies based on Fig. 5, in which three control strategies are compared.

As shown in Fig. 5, the original ACSC-based VCI has no effect at harmonic frequencies in case it is connected to a

distorted utility grid. Although the parallel resonant voltage controllers are often used at the primary level in islanded MGs to improve power quality, they increase harmonic admittance when the MG is connected to the utility grid. As shown in Fig. 5, the admittance of feed-in grid current with parallel resonant voltage controllers that significantly increase at harmonic frequencies, thereby indicating that the adopted resonant voltage controllers will deteriorate the power quality of feed-in grid current. By contrast, harmonic admittance can be effectively reduced with the proposed feed-in grid harmonic current compensation loop as indicated by the blue line in Fig. 5. The decreased harmonic admittance will induce more damping performance at harmonic frequencies, thereby effectively mitigating feed-in grid harmonic current of GCMG.

IV. Simulation and Experimental Results

A. Simulation results

A simulation model is built in MATLAB/Simulink to verify the proposed feed-in grid harmonic current suppression strategy. The simulation model includes two ACSC-based parallel VCIs with the proposed compensator, two resistive local loads, a resistive grid-side load and a distorted utility grid. The control and electrical parameters of the simulation model are shown in Table I.

Different harmonic components of the distorted grid voltage in the simulation model are shown in Table II, in

TABLE I
Electrical and Control Parameters for Simulation

		Parameters		Value
		Sym	Description	
Electrical Circuit		L_f	Filter Inductance	1.8 mH
		C_f	Filter Capacitance	9.9 μF
Loads		P_{local}	P of local load	800 W
		Q_{local}	Q of local load	400 Var
		P_{grid}	P of grid-side load	200 Var
		Q_{grid}	Q of grid-side load	50 Var
Primary	Inner Loops	k_{pv}	Voltage proportional term	0.04
		k_{iv}	Voltage resonant term	93.839
		k_{pi}	Current proportional term	0.07
	PLL	k_{pPLL}	PLL proportional term	1.4
		k_{iPLL}	PLL integral term	2000
	Virtual impedance	R_{vir1}	VR of inverter #1	1 Ω
		R_{vir2}	VR of inverter #2	2 Ω
	Harmonic compensator	k_{ihv}^{5th}	5th resonant term	10
		k_{ihv}^{7th}	7th resonant term	15
		k_{ihv}^{11h}	11th resonant term	20
Second-ary	Grid Synchronizati-on	$k_{p\omega\_grid}$	proportion term for ω	5e-3
		$k_{i\omega\_grid}$	integral term for ω	5e-5
		k_{pE_grid}	proportion term for E	10
		k_{iE_grid}	integral term for E	0.1
Tertiary	Grid-feeding controller	k_{pP}	Proportional term for P_{mg}	5e-2
		k_{iP}	Integral term for P_{mg}	5e-1
		k_{pQ}	Proportional term for Q_{mg}	8e-5
		k_{iQ}	Integral term for Q_{mg}	4e-4

TABLE II
Harmonic Components of Distorted Grid Voltage

	1st	5th	7th	11th
Positive	311 V	0.3 V	0.5 V	0.2 V
Negative	0 V	1 V	0.2 V	0.2 V

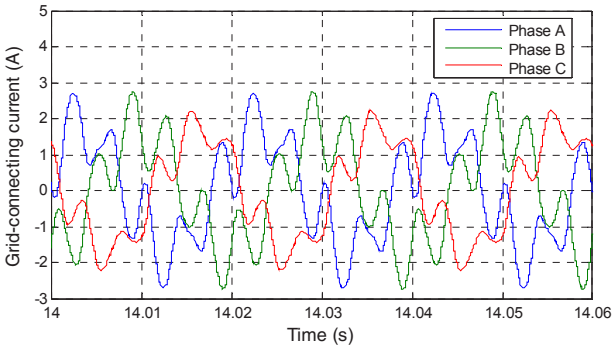

Fig. 6. Simulation results of the feed-in grid current in a GCMG only with the paralleled voltage PR controllers.

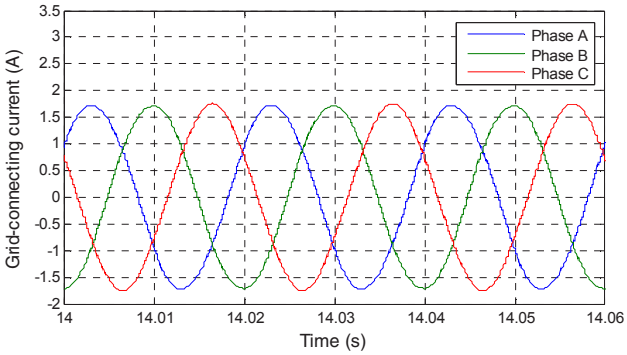

Fig. 7. Simulation results of the feed-in grid current in a GCMG with the proposed control strategy.

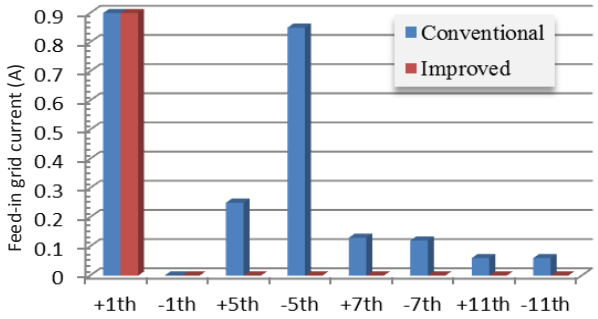

Fig. 8. Harmonic analysis comparison of feed-in grid currents.

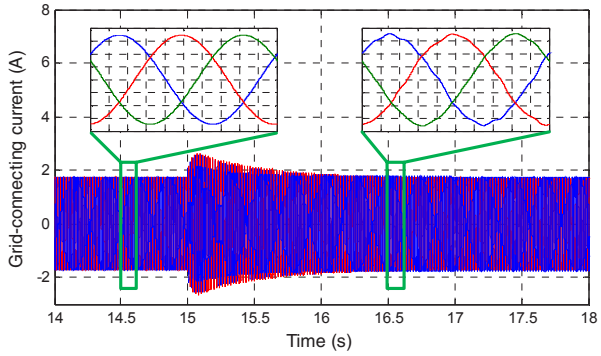

Fig. 9. Dynamic response of the GCMG with the proposed control strategy.

which the unbalanced low-frequency harmonic components are considered. The THD_v of PCC voltage is equal to 0.43%.

The simulation results of the feed-in grid current when the MG is connected to a distorted utility grid only with the parallel voltage resonant controllers are shown in Fig. 6. Evidently, small grid harmonic voltage results in seriously distorted feed-in grid current. The positive 5th, 7th, and 11th feed-in grid current components are equal to 0.25, 0.13, and 0.06 A. While the negative 5th, 7th, and 11th components are equal to 0.12, 0.12, and 0.06 A, respectively. The THD_i of feed-in grid current is 58.97 % which is significantly higher than the limit in grid code, such as IEEE Standard 929-2000.

In comparison, the THD_i of feed-in grid current in a GCMG with the proposed compensation loop is effectively improved, as shown in Fig. 7. Zero steady-state error for feed-in grid harmonic current compensation loop is achieved at each harmonic frequency. A detailed comparison is shown in Fig. 8.

Figure 9 shows the transient response of GCMG with the proposed harmonic compensation loop in case the grid voltage is suddenly distorted by a grid-side nonlinear load. In the beginning, a two VCI-based GCMG with the proposed feed-in grid harmonic current compensation loop is connected to an ideal grid, feeding around 500 W of active power and 200 Var of reactive power to the utility grid because of the power flow control at the tertiary level. At 15 s, the utility grid is distorted by adding a harmonic voltage source to emulate a grid-side nonlinear load disturbance, as shown in Table II. As observed in Fig. 9, after around 1.5 s, the feed-in grid current with the proposed harmonic compensator returns back to the stable operating point.

B. Experimental results

To verify the validity of the proposed feed-in grid harmonic current compensation loop, experiments on a three-VCI-based MG were conducted. The setup consisted of three Danfoss 2.2 kW inverters, a real-time dSPACE1006 platform, *LC* filters, a resistive local load, and a resistive grid-side load, as shown in Fig. 10. One of the VCIs was used to simulate the distorted utility grid. The proposed harmonic current compensator was implemented in the other two units to simulate the GCMG. The electrical setup and control system parameters are listed in Table III.

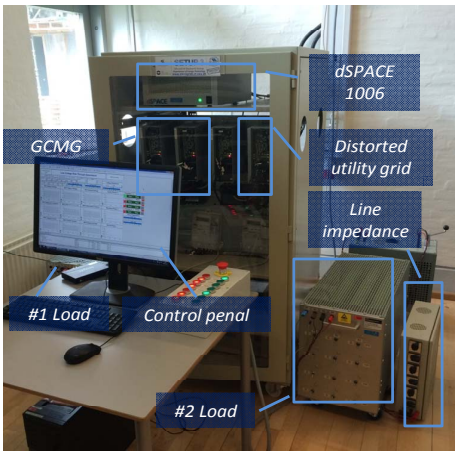

Fig. 10. Experimental setup

TABLE III
POWER STAGE PARAMETERS

	Description	Value
V_{dc}	DC voltage	650 V
V_{MG}	MG voltage	311 V
f	MG frequency	50 Hz
f_s	Switching frequency	10 kHz
L_f	Filter inductance	1.8 mH
C_f	Filter capacitance	25 μF
L_{line}	Resistive – inductive line	1 Ω + 1.7 mH
R_L	Local load	115 Ω

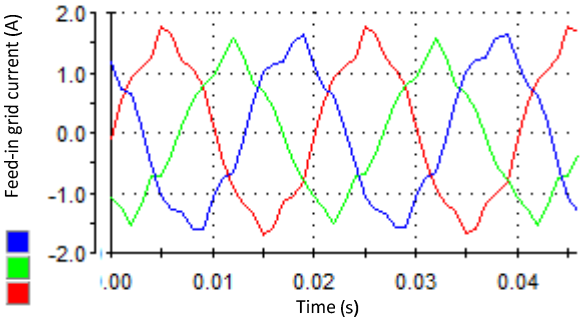

Fig. 11. Experimental results of the feed-in grid current in a GCMG only with the paralleled voltage PR controllers.

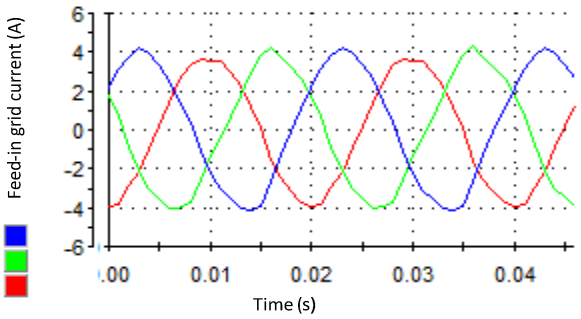

Fig. 12. Experimental results of the feed-in grid current in a GCMG with the proposed control strategy.

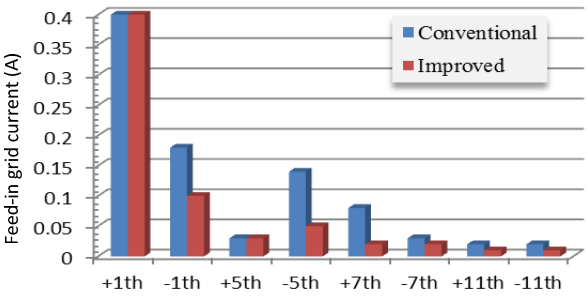

Fig.13. Harmonic analysis comparison of the experimental feed-in grid current.

The experimental results of the feed-in grid current in a GCMG only with the parallel voltage resonant controllers are shown in Fig. 11. The positive 5th, 7th, and 11th of feed-in grid harmonic current components are equal to 0.03, 0.08, 0.02 A. The negative 1st, 5th, 7th, and 11th harmonic

components are equal to 0.18, 0.14, 0.03, and 0.02A, respectively. The THD_i of feed-in grid current is 9.68%.

Figure 12 shows the experimental results of a GCMG with the proposed feed-in grid harmonic current compensation loop. In this case, the positive 5^{th}, 7^{th}, and 11^{th} feed-in grid harmonic current components are reduced to 0.03, 0.02, 0.01 A. Meanwhile, the negative 1^{st}, 5^{th}, 7^{th}, and 11^{th} harmonic components are reduced to 0.1, 0.05, 0.02, and 0.01 A respectively, thanks to the proposed controller. The THD_i of the feed-in grid current is effectively mitigated to 2.97%. The detailed comparative results are shown in Fig. 13.

V. CONCLUSION

A novel feed-in grid harmonic current suppression control strategy for GCMGs that is connected to a distorted utility grid is proposed in this paper. The system equivalent output admittance can be effectively reduced at selected harmonic frequencies because of the feed-in grid current resonant controller-based harmonic compensation loop and the parallel resonant controllers in the voltage control loop. Finally, the total harmonic distortion of feed-in grid current can be significantly decreased. Simulation and experimental results from a three 2.2 kW VCIs-based GCMG are shown to verify the effectiveness of the proposed controller.

ACKNOWLEDGMENT

The authors appreciate the supports by the project of Open virtual neighborhood network to connect intelligent buildings and smart objects (VICINITY) (GA# 688467), funded by the European Commission (EC) Directorate-General for Research and Innovation (DG RTD), under the ICT-30 IoT action of its Horizon 2020 Research and Innovation Programme (H2020).

REFERENCES

[1] Hatziargyriou, N., Asano, H., Iravani, R., Marnay, C.Microgrids, "MicroGrids," *Power and Energy Magazine, IEEE on*, vol. 5, no. 4, pp. 78-94, Jul. 2007

[2] U. Borup, F. Blaabjerg, and P. Enjeti, "Sharing of nonlinear load in parallel-connected three-phase converters," *IEEE Trans. Ind. Appl*., vol. 37, no. 6, pp. 1817–1823, Nov./Dec. 2001.

[3] T. L. Lee and P. T. Cheng, "Design of a new cooperative harmonic filtering strategy for distributed generation interface converters in an islanding network," *IEEE Trans. Power Electron*., vol. 22, no. 5, pp. 1919–1927, Sep. 2007.

[4] P. T. Cheng, C. A. Chen, T. L. Lee, and S. Y. Kuo, "A cooperative imbalance compensation method for distributed-generation interface converters," *IEEE Trans. Ind. Appl*., vol. 45, no. 2, pp. 805–815, Mar./Apr. 2009.

[5] Jinwei He, YunWei Li, Josep M. Guerrero, Frede Blaabjerg, Juan C. Vasquez, "An Islanding Microgrid Power Sharing Approach Using Enhanced Virtual Impedance Control Scheme," *IEEE Trans. Power Electron*., vol. 28, no. 11, pp. 5272–5282, Sep. 2013.

[6] Tzung-Lin Lee, Po-Tai Cheng, "Design of a New Cooperative Harmonic Filtering Strategy for Distributed Generation Interface Converters in an Islanding Network," *IEEE Trans. Power Electron*., vol. 22, no. 5, pp. 1919–1927, Sep. 2007.

[7] Josep M. Guerrero, José Matas, Luis García de Vicuña, Miguel Castilla, Jaume Miret, "Wireless-Control Strategy for Parallel Operation of Distributed-Generation Inverters," *Industrial Electronics, IEEE Transactions on*, vol.53, no.5, pp.1461-1470, Oct. 2006.

[8] Zhilei Yao and Lan Xiao, "Control of single-phase grid-connected inverters with nonlinear loads," *IEEE Trans. on Ind. Electron*., vol. 60, no. 4, pp. 1384–1389, Apr. 2013.

[9] Xiaoqiang Guo, Wenzhao Liu, Xue Zhang, Xiaofeng Sun, Zhigang Lu, Josep M. Guerrero. "Flexible Control Strategy for Grid-Connected Inverter Under Unbalanced Grid Faults Without PLL," *IEEE Transactions on Power Electronics*, vol. 30, no. 4, pp. 1773–1778, July 2014.

[10] Jinwei He, Yun Wei Li, Munir, M.S, "A Flexible Harmonic Control Approach through Voltage-Controlled DG–Grid Interfacing Converters," *Industrial Electronics, IEEE Transactions on*, vol. 59, no. 1, pp. 444-455, Apr. 2011.

[11] Jinwei He, Yun Wei Li, Blaabjerg, F., "Flexible Microgrid Power Quality Enhancement Using Adaptive Hybrid Voltage and Current Controller," *Industrial Electronics, IEEE Transactions on*, vol. 61, no. 6, pp. 2784-2794, Sep. 2013.

[12] Xiongfei Wang, Frede Blaabjerg, "Harmonic Stability in Power Electronic Based Power Systems: Concept, Modeling, and Analysis," *IEEE Transactions on Smart Grid*, vol., no., pp., 2018.

[13] Jinwei He, Beihua Liang, "Direct Microgrid Harmonic Current Compensation and Seamless Operation Mode Transfer Using Coordinated Triple-Loop Current-Voltage-Current Controller," *IEEE 8th International Power Electronics and Motion Control Conference*, 2016 , IPEMC-ECCE Asia, May 2016.

[14] Y. A. Ibrahim Mohamed, E. F. El-Saadany. "Adaptive Decentralized Droop Controller to Preserve Power Sharing Stability of Paralleled Inverters in Distributed Generation Microgrids," *IEEE Transactions on Power Electronics*, vol. 23, no. 6, pp.2806-2816, Nov. 2008.

[15] N. Pogaku, M. Prodanovic, and T. C. Green, "Modeling, analysis and testing of autonomous operation of an inverter-based microgrid," *IEEE Trans. Power Electron*., vol. 22, no. 2, pp. 613–625, Mar. 2007.

[16] Guan, Y., Guerrero, J.M., Zhao, X., Vasquez, J.C., Guo, X. "A New Way of Controlling Parallel-Connected Inverters by Using Synchronous-Reference-Frame Virtual Impedance Loop—Part I: Control Principle," *Power Electronics, IEEE Transactions on*, vol. 31, no. 6, pp: 4576 - 4593, June. 2016.

[17] Yajuan Guan, Juan C. Vasquez, Josep M. Guerrero, "Hierarchical controlled grid-connected microgrid based on a novel autonomous current sharing controller," *Energy Conversion Congress and Exposition (ECCE)*, 2015 IEEE, Sept. 2015, Montreal.